International Journal of Solids and Structures 50 (2013) 4341–4348

Contents lists available at ScienceDirect

International Journal of Solids and Structures

journal homepage: www.elsevier.com/locate/ijsolstr

Analytical formulations of image forces on dislocations with surface stress in nanowires and nanorods

Wei Ye, Abdallah Ougazzaden, Mohammed Cherkaoui *

Georgia Institute of Technology, Atlanta, GA 30332, USA
GTL, UMI 2958 Georgia Tech-CNRS, Metz 57070, France

ARTICLE INFO

Article history:
Received 25 April 2013
Received in revised form 24 July 2013
Available online 13 September 2013

Keywords:
Dislocation
Image force
Surface stress
Nanowire
Nanorod

ABSTRACT

The interaction between dislocations and surfaces is usually characterized by image forces. Most analytical solutions to image forces could be found in literatures for two-dimensional (2D) solids with or without the consideration of surface stress. This work provides alternative analytical formulations of image forces for nanowires which are in more flexible forms compared with the infinite power series solutions from complex variable method. Moreover, this work proposes analytical formulations of image forces for nanorods (3D) by approximating the 3D shape effect as a height-dependent shape function, which is obtained through curve fitting of the finite element results of image forces without surface stress. The results of nanowires are demonstrated to be acceptable compared with the classical solution and complex variable method. More importantly, the analytical formulation of nanorods has not been found in other literatures so far. This work could contribute to nanostructure design and provide guidance for the fabrication of high quality nanostructures.

Published by Elsevier Ltd.

1. Introduction

Dislocations in solids play an important role in determining the mechanical and electronic properties of materials (Du and Srolovitz, 2004; Liu et al., 2004; Luryi and Suhir, 1986; People and Bean, 1985; Schwarz, 1999; Srinivasan et al., 2003; Zhong and Zhu, 2008), due to the fact that the atoms of the dislocations have different bonding and environment from the other atoms buried in the bulk. More importantly, when the dislocation is embedded in nanostructures with dimensions on the order of tens of nanometers, the behavior of the dislocation becomes highly sensitive to the surrounding environment because the atoms near the dislocation will interact more actively in such extremely small domain. Generally, external loads, grain boundaries, inclusions and surfaces/interfaces, etc. will affect the behavior of the dislocation. This influence might be crucial in determining the way that the dislocation behaves in nanostructures, thus it should be taken into consideration in comprehensive studies.

Classical studies (Hirth and Lothe, 1982; Hull and Bacon, 2011) showed that a fictitious image dislocation needs to be imposed to enforce the stress-free surface boundary condition when a dislocation is embedded in a semi-infinite solid. The image dislocation has the same magnitude but opposite direction of the Burgers vector of the original dislocation. Based on the concept of the image dislocation, Dundurs and coworkers (Dundurs and Mura, 1964; Dundurs and Sendeckyj, 1965) studied the elastic fields and image forces with the consideration of the interaction between an edge dislocation and a circular inclusion. Lubarda (2011) obtained the stress fields for screw and edge dislocations emitted from a cylindrical void and provided analytical formulations for image forces on dislocations. A different scheme to analyze the displacement and strain fields of a screw dislocation in a nanowire is by using gradient elasticity theory (Aifantis, 2003, 2009, 2011; Davoudi et al., 2009, 2010; Shodja et al., 2008). They provide more complete solutions for non-singular stresses and strains in dislocations compared with the classical nonlocal approach (Eringen, 1977, 1984, 2001). It was employed to derive the solution to the image force in an integral form on a screw dislocation near a flat interface (Gutkin et al., 2000). The study of dislocations in gradient elasticity theory was revisited and extended by Lazar and coworkers (Lazar and Maugin, 2006; Lazar et al., 2006) to the second gradient elasticity theory to analyze the stress and strain field of the edge or screw dislocation. Another distinct approach to investigate image forces acted on dislocations is through the complex variable method or complex potential method (Muskhelishvili, 1977). This approach is based on the analogy (Smith, 1968) between the anti-plane strain deformation and the 2D perfect fluid motion, so it is mainly used in 2D situations. Smith (1968) pioneered to study the interaction between screw dislocations and circular cylindrical inhomogeneities. By using conformal transformation techniques, elliptical inclusions were considered by Stagni and Lizzio (1983)

* Corresponding author.
E-mail address: mcherkaoui@me.gatech.edu (M. Cherkaoui).

0020-7683/$ - see front matter Published by Elsevier Ltd.
http://dx.doi.org/10.1016/j.ijsolstr.2013.09.007

for the dislocation in the matrix and Warren (1983) for the dislocation in the inclusion. Moreover, anisotropy was also taken into consideration through Stroh's formalism (Stroh, 1958) and image forces on dislocations in anisotropic elastic half-spaces with a fixed boundary was obtained by Ting and Barnett (1993). However, in these mentioned formulations and many more, there is no intrinsic length scale associated in these constitutive relationships. Therefore, these results should be considered only in macroscopic cases.

In the past few decades, nanotechnology has been developed rapidly and it discloses that the behaviors of nano-materials differ from the conventional materials dramatically. Nanostructures have at least one of its dimensions below tens of nanometers. Due to the large surface to volume ratio, the surface stress begins to play an important role in changing the constitutive laws seen in the classical elastic theory. In this case, nanostructures usually demonstrate some size-dependent properties that could not be seen in conventional materials. This significant difference could be critical in fabrications and designs, so great efforts have been devoted to investigating the effect of surface stress. Relationship of the deformation-dependent surface energy with the surface stress was first described by the Shuttleworth's equation (Shuttleworth, 1950). Gurtin and coworkers (Gurtin and Ian Murdoch, 1975; Gurtin et al., 1998) linked the surface stress to the bulk stress at the vicinity of the surface by regarding the surface as a negligibly thin object adhering to the underlying material without slipping. Aifantis et al. (2007) adopted the strain gradient approach for nucleation of misfit dislocations and plastic deformations in core/shell nanowires. They also considered the interface contribution to the gradient dependent potential energy of polycrystals in terms of interfacial strain (Aifantis and Askes, 2007). Fang and Liu (2006a,b) combined the surface stress model with complex variable method to solve the image force for a screw or edge dislocation located in materials of a circular nanowire embedded in an infinite matrix. Luo and Xiao (2009) extended this analysis to the case of an elliptical nanowire embedded in an infinite matrix with conformal mappings. Recently, Ahmadzadeh-Bakhshayesh et al. (2012) adopted the same method to analyze the surface/interface effect on the image force of a screw dislocation in an eccentric core–shell nanowire. However, these results based on the complex variable method provide the results of image forces as infinite power series, which are difficult to manipulate in further situations. The influences of the size parameter and surface elasticity are also hard to interpret clearly. Beside this limitation, their solutions by using the complex variable method are limited to 2D elastic plane stress or strain problems and mainly used for isotropic materials.

2. General formulation of image force

The calculation of the image force mainly falls into two categories: the nonlocal approach and the energy approach. The "nonlocal" concept was introduced by Kröner (1967) and followed by Eringen (1977, 1984, 2001) to tackle the mathematical singularity due to the discrete field of dislocations. In the nonlocal approach, one can calculate the image force along the dislocation line using the Peach–Koehler equation (Hirth and Lothe, 1982):

$$\vec{f} = (\sigma^{NL} \bullet \vec{b}) \times \vec{\xi}, \tag{1}$$

where $\vec{f}$ is the image force density vector along the dislocation line, σ^{NL} is the nonlocal stress exerted on the dislocation, and $\vec{\xi}$ is the unit vector along the direction of the dislocation line.

The nonlocal stress requires a volumetric integration of the stress tensor over the whole crystal space (Kröner, 1967):

$$\sigma^{NL}(\vec{x}) = \int_V \kappa(\vec{x} - \vec{x}')\sigma(\vec{x}')dV', \tag{2}$$

where $\kappa(\vec{x} - \vec{x}')$ is a correlation kernel that links the local point $(\vec{x})$ on the dislocation line to the nonlocal point $(\vec{x}')$ in the rest crystal space.

The nonlocal stress σ^{NL} should be the sum of the contribution from all other portions of the crystal to the dislocation, which accounts for the long range effects from the free surfaces. Usually a volumetric integration over the whole crystal space should be calculated for σ^{NL}.

Recently, Colby et al. (2010) investigated the dislocation filtering behavior in GaN nanodots by selective area growth through a nanoporous template. This dislocation dissipation mechanism has been studied numerically through finite element method based on the nonlocal approach (Liang et al., 2010; Ye et al., 2012), in which the surrounding surfaces are considered only as free surfaces and the evaluation the nonlocal stress in Eq. (2) only considers the largest contribution from the linear integral of the stress part in the plane perpendicular to the dislocation.

The energy approach is based on the virtual work principle. In mechanics, a general force is defined as the change of the total energy relative to a general configuration coordinate change:

$$f = -\frac{\partial W}{\partial a}, \tag{3}$$

where ∂a can be seen as the change of the dislocation position in this case, and W is the total energy stored in the solid.

Similar to the nonlocal approach, the calculation of the total energy usually requires a volumetric integration of the energy density over the whole crystal space. This is quite cumbersome in most cases and it is often approximated as the same energy to introduce the dislocation into the crystal (Ahmadzadeh-Bakhshayesh et al., 2012; Dundurs and Mura, 1964; Dundurs and Sendeckyj, 1965; Fang and Liu, 2006a, b; Luo and Xiao, 2009). The approximation is carried out by evaluating the work done by stresses on the cut surface of the dislocation to move the slip plane. It could avoid the energy integration directly but somehow neglect the stress contributions from other part of the material.

This work adopts the energy approach to formulate analytically image forces on dislocations with surface stress in nanowires and nanorods. First, the analytical stress and strain fields are derived in case of isotropic circular nanowires. The results are fed into the energy approach to obtain the analytical formulation of image forces of nanowires. Second, this work proposes to study image forces of nanorods by approximating the 3D shape effect as a height-dependent shape function, which could be obtained through curve fitting of the finite element data without surface stress. This work provides explicitly analytical formulations of image forces on dislocations in nanowires and nanorods with surface stress. The results of nanowires are demonstrated to be acceptable compared with the classical solution and complex variable method. More importantly, the analytical formulation of nanorods has not been found in other literatures so far. This work could contribute to nanostructure design and provide guidance for the fabrication of high quality nanostructures.

3. Stress field

In Fig. 1, consider an elastic solid of domain (V) with an inclusion (Ω) prescribed with an eigenstrain ε^*. The surface of the solid is denoted by (S).

The constitutive relationship of the stress and the strain is:

$$\sigma_{ij} = L_{ijkl}(\varepsilon_{kl} - \varepsilon^*_{kl}), \tag{4}$$

where L_{ijkl} is the stiffness tensor of the material.

The strain is related to the displacement through compatibility condition:

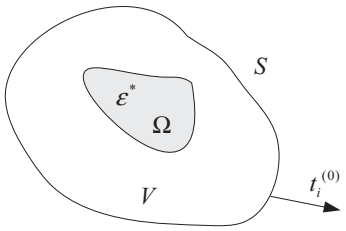

Fig. 1. An elastic solid of domain (V) with an inclusion (Ω) prescribed with an eigenstrain.

$$\varepsilon_{ij} = \frac{1}{2}\left(u_{i,j} + u_{j,i}\right). \tag{5}$$

When surface stress is concerned, the bulk stress state at the vicinity of the surface is determined from the surface stress (Gurtin and Ian Murdoch, 1975; Gurtin et al., 1998):

$$\sigma^s_{\alpha\beta,\beta} + \sigma^b_{\alpha\beta} n_\beta = 0, \tag{6}$$

$$\sigma^s_{\alpha\beta}\kappa_{\alpha\beta} = \sigma^b_{ij} n_i n_j, \tag{7}$$

where $\sigma^s_{\alpha\beta}$, $\sigma^b_{\alpha\beta}$ are the surface stress and bulk stress respectively and $\kappa_{\alpha\beta}$ is the curvature tensor.

It should be noted that the surface stress tensor is a two-dimensional quantity and the strain normal to the surface is excluded. Thus, the Greek indices take the value of 1 or 2, while Latin subscripts adopt values from 1 to 3.

Consider a linear constitutive relationship between surface stress and surface strain as (Miller and Shenoy, 2000):

$$\sigma^s_{\alpha\beta} = \tau^0_{\alpha\beta} + S_{\alpha\beta\gamma\delta}\varepsilon^s_{\gamma\delta}, \tag{8}$$

where $\tau^0_{\alpha\beta}$ is the residual surface stress when the bulk is unstrained, $S_{\alpha\beta\gamma\delta}$ is the elastic constants for the surface that can be determined from atomistic calculations. $\varepsilon^s_{\gamma\delta}$ is the surface strain that only accounts for in-plane deformation usually.

An alternative expression of Eq. (8) is given in terms of surface excess energy (Dingreville et al., 2005):

$$\Gamma = \Gamma_0 + \Gamma^{(1)} : \varepsilon^s + \frac{1}{2}\varepsilon^s : \Gamma^{(2)} : \varepsilon^s, \tag{9}$$

where Γ is the surface excess energy, and $\Gamma_0, \Gamma^{(1)}, \Gamma^{(2)}$ are the surface property tensors ($\Gamma^{(1)}$ is equivalent to $\tau^0_{\alpha\beta}$ and $\Gamma^{(2)}$ is equivalent to $S_{\alpha\beta\gamma\delta}$).

Equations (4)–(8) demonstrate a general analytical framework to solve the elastic field for solids with defects by considering surface effect. Compared to the limitations of complex variable method, this framework is applicable to anisotropic materials and 3D structures. More importantly, it allows for the exact analytical expression of the results instead of the power series solution in complex variable method. Such exact analytical expressions of the stress or strain field will be more flexible to manipulate in further applications.

For the present, consider a straight screw dislocation with Burgers vector $\vec{b} = [0, 0, b]$ oriented in $\langle 0\,0\,1\rangle$ direction in the nanowire (Fig. 2). The radius of the nanowire is R and the dislocation is located on x_1-axis with an offset of a from the center ($\delta = a/R$). The bulk material elastic constants are denoted by μ as the shear modulus and υ as the Poisson's ratio. The surface elasticity is also considered to be isotropic and the surface constitutional relationship is simplified as (Gurtin and Ian Murdoch, 1975):

$$\sigma^s_{\alpha\beta} = \tau^0\delta_{\alpha\beta} + 2\left(\mu^0 - \tau^0\right)\varepsilon_{\alpha\beta} + \left(\lambda^0 + \tau^0\right)\varepsilon_{\gamma\gamma}\delta_{\alpha\beta}, \tag{10}$$

where μ^0 and λ^0 are the surface Lamé constants; $\delta_{\alpha\beta}$ is the Kroneker delta tensor.

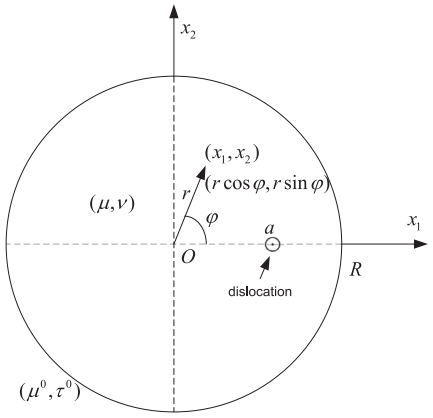

Fig. 2. Cross section view of the nanowire with a screw dislocation.

Under the superposition principle, the stress field is considered to consist of two parts:

$$\sigma_{ij} = \sigma^1_{ij} + \sigma^2_{ij}, \tag{11}$$

where σ^1_{ij} is the stress field due to free surface effect and σ^2_{ij} is the stress field due to surface stress.

Only shear components of the stress tensors are considered, as the same case dealt in the complex variable method. The first stress part is the same with the classical stress solution of the dislocation in the same nanowire but due to free surface (Hirth and Lothe, 1982):

$$\sigma^1_{13} = -\frac{\mu b}{2\pi}\left(\frac{x_2}{(x_1 - a)^2 + x_2^2} - \frac{x_2}{\left(x_1 - \frac{R^2}{a}\right)^2 + x_2^2}\right), \tag{12}$$

$$\sigma^1_{23} = \frac{\mu b}{2\pi}\left(\frac{x_1 - a}{(x_1 - a)^2 + x_2^2} - \frac{x_1 - \frac{R^2}{a}}{\left(x_1 - \frac{R^2}{a}\right)^2 + x_2^2}\right). \tag{13}$$

The second stress part due to surface stress is solved as (Ye et al., 2013):

$$\sigma^2_{13} = \frac{ab\sin(\varphi)\cos(\varphi)\left(R^2 - a^2\right)}{\pi\left(R^2 + a^2 - 2Ra\cos(\varphi)\right)^2}\frac{r}{R^2}\left(\mu^0 - \tau^0\right), \tag{14}$$

$$\sigma^2_{23} = \frac{ab\sin(\varphi)\sin(\varphi)\left(R^2 - a^2\right)}{\pi\left(R^2 + a^2 - 2Ra\cos(\varphi)\right)^2}\frac{r}{R^2}\left(\mu^0 - \tau^0\right). \tag{15}$$

The stress field has been checked with the classical solution and complex variable method (Ye et al., 2013). They agree well with each other generally and it is demonstrated that surface stress only has an important influence on the final stress field when the radius of the nanowire is small enough. The stress component of σ_{23} from complex variable method conflicts from the classical solution when the size of the nanowire becomes sufficiently large (R = 100 nm) while the result from this work shows a better correspondence. In the following, image forces will be derived based on the stress field given in Eq. (11).

4. Image force of nanowire

With the stress solution, image forces of nanowires could be obtained through the energy approach in Section 2. As a 2D case, the total energy per unit length of the nanowire is given as:

$$W = W_b + W_s, \tag{16}$$

where W_b is the elastic strain energy stored in the bulk material, and W_s is the surface excess energy.

In continuum mechanics, the bulk elastic strain energy per unit length is:

$$W_b = \int_s \frac{1}{2}\sigma_{ij}\varepsilon_{ij}ds = \int_s \frac{1}{2\mu}\left[(\sigma_{13}^1)^2 + (\sigma_{23}^1)^2 + (\sigma_{13}^2)^2 + (\sigma_{23}^2)^2 + 2\sigma_{13}^1\sigma_{13}^2 + 2\sigma_{23}^1\sigma_{23}^2\right]ds. \tag{17}$$

For convenience, it can be rewritten as three parts:

$$W_b = W_1 + W_2 + W_3, \tag{18}$$

where

$$W_1 = \int_s \frac{1}{2\mu}\left[(\sigma_{13}^1)^2 + (\sigma_{23}^1)^2\right]ds, \tag{19}$$

$$W_2 = \int_s \frac{1}{2\mu}\left[2\sigma_{13}^1\sigma_{13}^2 + 2\sigma_{23}^1\sigma_{23}^2\right]ds, \tag{20}$$

$$W_3 = \int_s \frac{1}{2\mu}\left[(\sigma_{13}^2)^2 + (\sigma_{23}^2)^2\right]ds. \tag{21}$$

The corresponding image force contribution (f_1, f_2, f_3) due to these three parts can be obtained from the energy approach of Eq. (3). Note that W_1 is the same energy of the classical case of free surfaces, so f_1 is the same as the image force of the classical situation (Eshelby, 1953; Hirth and Lothe, 1982):

$$f_1 = \frac{\mu b^2}{2\pi}\frac{a}{R^2 - a^2}. \tag{22}$$

Another two image force parts are obtained after some tedious calculations directly:

$$\begin{aligned} f_2 = &-\frac{b^2(\mu^0 - \tau^0)}{\left(a^4 - 2R^2a^2 + R^4\right)R^5a^5\pi} \\ &\times\Big[(4\ln(a+R) - 8\ln(R) + 4\ln(R-a))R^{12} \\ &+(-8\ln(R-a)a^2 - 8\ln(a+R)a^2 + 16\ln(R)a^2 + 4a^2)R^{10} \\ &+(4\ln(R-a)a^4 + 4a^4\ln(a+R) - 6a^4 - 8a^4\ln(R))R^8 \\ &+2R^6a^6 - a^7R^5 + (4a^8\ln(a+R) - 2a^8 - 4a^8\ln(a))R^4 \\ &+7a^9R^3 + (2a^{10} + 8a^{10}\ln(a) - 8a^{10}\ln(a+R))R^2 - 4Ra^{11} \\ &-4a^{12}\ln(a) + 4a^{12}\ln(a+R)\Big], \end{aligned} \tag{23}$$

$$f_3 = -\frac{ab^2\left(R^4 + a^4 + 4R^2a^2\right)}{4\pi\mu\left(R^2 - a^2\right)^4}(\mu^0 - \tau^0)^2. \tag{24}$$

From Eq. (9), the surface excess energy per unit length of the nanowire is given as:

$$W_s = \int_s \Gamma ds = \int_s \left(\Gamma_0 + \Gamma^{(1)} : \varepsilon^s + \frac{1}{2}\varepsilon^s : \Gamma^{(2)} : \varepsilon^s\right)ds. \tag{25}$$

The corresponding image force part due to the surface excess energy is:

$$f_4 = -\frac{\partial W_s}{\partial a} = -\int_s \left(\Gamma_{ij}^{(1)}\frac{\partial \varepsilon_{ij}^s}{\partial a} + \Gamma_{ijkl}^{(2)}\frac{\partial \varepsilon_{ij}^s}{\partial a}\varepsilon_{kl}^s\right)ds. \tag{26}$$

From Eqs. (8) and (10), it can be simplified to:

$$f_4 = -\int_s \frac{1}{2(\mu^0 - \tau^0)}\frac{\partial \varepsilon_{ij}^s}{\partial a}\varepsilon_{ij}^s ds, \tag{27}$$

where ε_{ij}^s is the same with the bulk strain for coherent surfaces and the bulk strain can be obtained from the known stress field.

Using Eq. (11) and Hooke's Law, we obtain the last image force part:

$$f_4 = -\frac{Rab^2(\mu^0 - \tau^0)}{\pi\left(a^4 - 2R^2a^2 + R^4\right)}. \tag{28}$$

Finally, we obtain the analytical solution to the image force of isotropic circular nanowire:

$$f = f_1 + f_2 + f_3 + f_4. \tag{29}$$

When the surface elasticity is set to zero, our solution is reduced to the classical solution in Eq. (22). By contrast, the image force solution of complex variable method is given as infinite power series (Liu and Fang, 2007):

$$f = \frac{\mu b^2}{2\pi}\sum_{k=0}^{\infty}\frac{\mu - (1+k)\frac{\mu^0 - \tau^0}{R}}{\mu + (1+k)\frac{\mu^0 - \tau^0}{R}}\frac{a^{2k+1}}{R^{2k+2}}. \tag{30}$$

It can be seen directly that Eq. (30) has the problem with the denominator when the surface elasticity $\mu^0 - \tau^0$ becomes negative, which makes it close to zero for a certain k value. This will lead the solution of complex variable method to abrupt fluctuations and to avoid this instability, summation terms need to be selected carefully.

Fig. 3 shows the image forces of dislocation inside an isotropic nanowire obtained from different solutions. For the case of negative surface elasticity, our solution agrees well with that of complex variable method and both solutions shows obvious differences from the classical solution when the size of the nanowire is below 10 nm. The image force also behaves as expected for the nanowire with a large size as it reduces to the classical solution. This means the surfaces stress only plays an important role in determining the image force in nano-scale and it can be negligible in macro-scale. However, as for the case of positive surface elasticity, our solution shows a different tendency as the image force abruptly goes to negative values when the radius of the nanowire becomes smaller than 5 nm. This tendency is opposite to that of the classical solution and complex variable method in this case.

A more comprehensive investigation of this deviation is shown in Fig. 4. It is found out that our solution with positive surface elasticity still agrees well with the classical solution and complex variable method in some cases. The deviation only happens when the dislocation is close to the surface ($\delta > 0.5$) and the radius of the nanowire is extremely small ($R < 3$ nm). Generally, the interaction between the dislocation and the surface should become more intense in smaller nanowires when the dislocation is closer to the surface. Especially the extremely small nanowires ($R < 3$ nm)

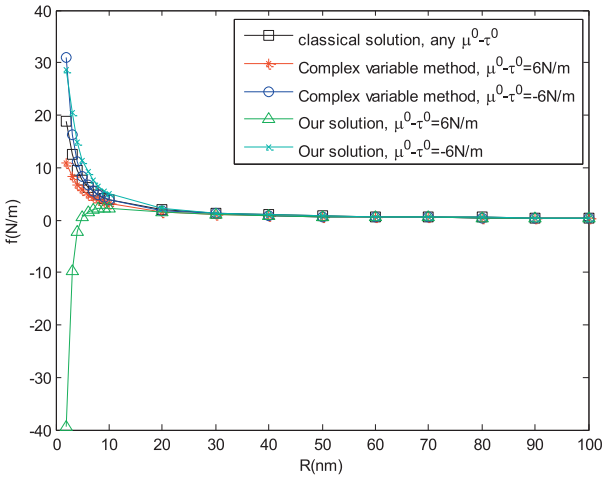

Fig. 3. Image forces of dislocation inside an isotropic nanowire.

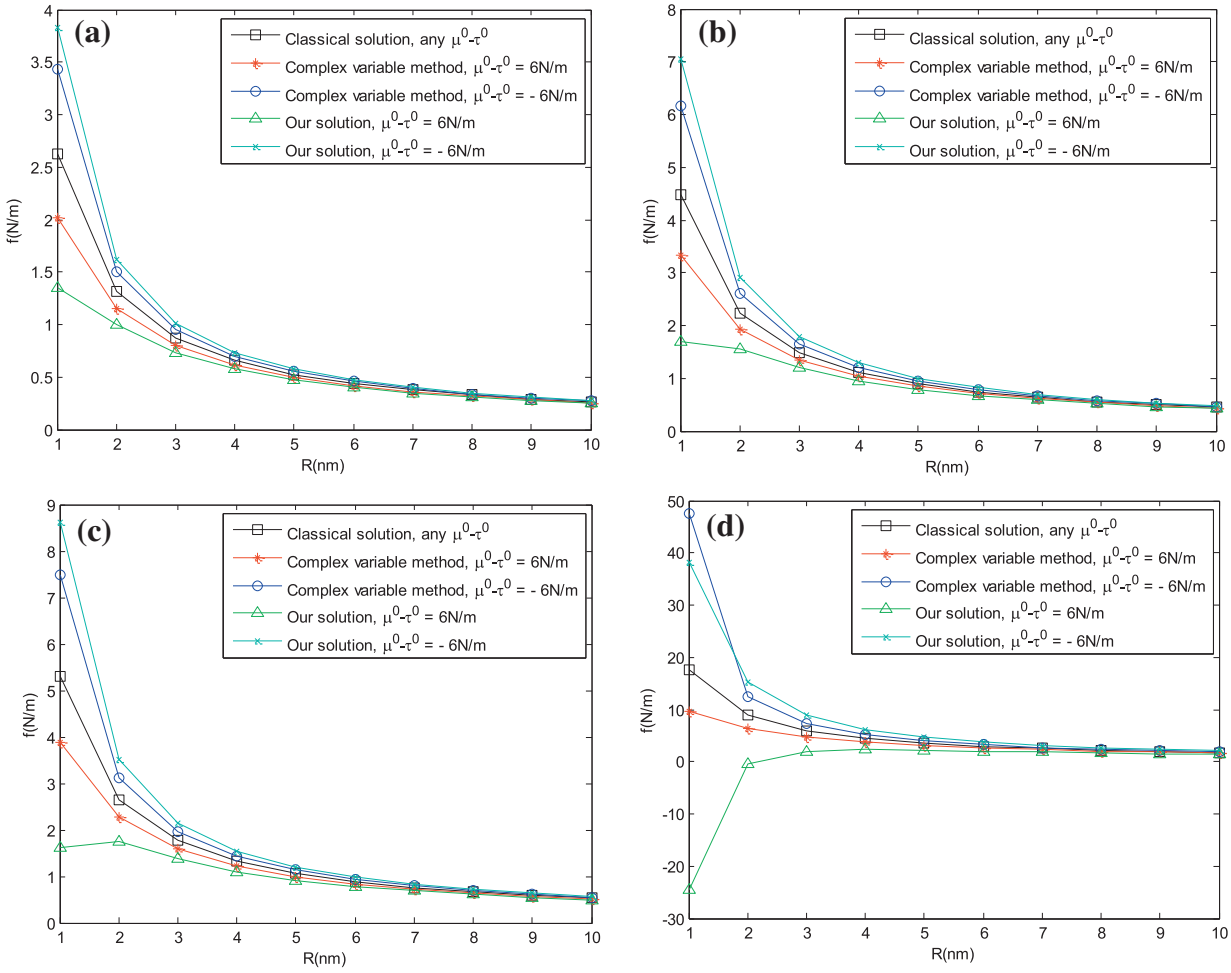

Fig. 4. Image forces of dislocation inside an isotropic nanowire with different offsets (a. $\delta = 0.3$; b. $\delta = 0.45$; c. $\delta = 0.5$; d. $\delta = 0.8$).

are in fact composed of only tens of atomic layers in terms of atomistic aspect, so the behavior of the image force becomes quite sensitive with the environment. Due to the lack of other corroborations from literatures to validate different approaches, the calculation of image force for dislocations with surface stress is still an open question. The complex variable method shows good results of image forces compared with the classical ones, but it is derived from the stress field which is shown to be against the common sense of mechanics in case of large nanowires. On the other hand, our work provides an alternative formulation of the image force based on the stress field which has been checked to be agreeable with the classical one and it also has good correspondence with complex variable method. Our solution of the image force is also acceptable compared with the classical solution and complex variable method except the case of positive surface elasticity and the deviation only happens when the dislocation is close to the surface and the radius of the nanowire is extremely small.

5. Image force of nanorod

In this work, the nanorod (finite cylinder) is taken as a special 3D nanostructure and image forces on dislocations in nanorods are investigated. Eqs. (4)–(8) demonstrate a general analytical framework to solve the elastic field for nanorods, but it is not feasible to obtain the exactly analytical solution directly. However, since it is possible to calculate image forces of dislocations without surface stress from finite element analysis (Liang et al., 2010; Ye et al., 2012), this work proposes to study image forces of nanorods by approximating the 3D shape effect as a height-dependent shape function, which could be obtained through curve fitting of the finite element data without surface stress. Finally, the same shape function is multiplied to the image force of nanowires with surface stress in Section 4, and the result could be compared with the original image forces of nanorods from finite element analysis.

Let us denote the image force of the isotropic circular nanowire by f_0 and that of the isotropic finite cylinder (nanorod) by f. When the two structures have the same radius R, the two image forces should behave as shown in Fig. 5.

According to St. Venant's principle, the surface effect of the two ends in the nanorod will only penetrate to a distance of order R, which is denoted as the effective length, h_e. Beyond the effective region, the image forces of nanowires and nanorods should be identical in the middle region. As an approximation, the corresponding image force of the nanorod could be determined as:

$$f = f_0 \times g(z), \tag{31}$$

where $g(z)$ is a height dependent shape function that only consists z coordinate.

In principle, the shape function of a particular nanorod should be distinct, which could be influenced by the geometry of the nanorod (radius and height), the material anisotropic orientation or even the effect of surface stress. To simplify the analysis, we only take account the longitudinal geometry feature for the shape

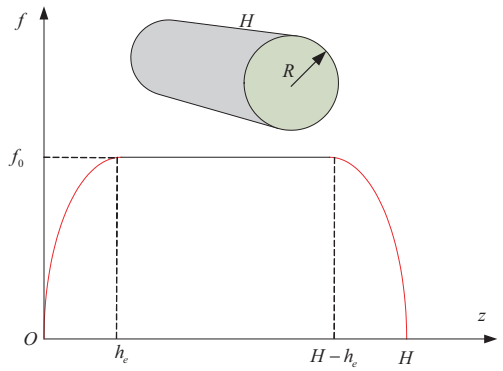

Fig. 5. Image forces of nanowire and finite cylinder (nanorod).

function in this work. In the following, we will obtain the shape function of the image force by curve fitting the finite element data, and this same shape function will be adopted for further study with surface stress.

By using the same methodology in finite element analysis (Ye et al., 2012), this work has calculated the image forces for three groups of nanorods with five different ratios between radius and height respectively (Fig. 6). Each group keeps the radius of the nanorod as a constant. It is quite straightforward to notice the plateau of the image force in the middle region of the nanorod when the height of the nanorod is obviously larger than the radius. Even for the case of short nanorods, the maximum image force at the middle point is very close to the longer nanorods. The comparison of the maximum image force from finite element analysis with that from the classical analytical solution is listed in Table 1.

Table 1 shows that there are some deviations between the finite element analysis and the classical analytical solution although both of them are calculated in the case of free surfaces (without surface stress). This might arise from the approximations made to facilitate the calculation of image forces as explained in Section 2. However, the ratio of the two results is quite consistent when the radius changes. In this way, we can add the average ratio value as a correction factor to Eq. (31). For our case, the correction factor is set to $\gamma = 1.797$.

Another important quantity to be determined from Fig. 6 is the effective length, h_e. It is instinctive to assume that the effective length should be proportional to the radius of the nanorod, since the shortest distance of the dislocation from the lateral free surface is close to R. In Fig. 6, the ratio of the effective length to the radius for long nanorods ($H > 4R$) is found to be constant, and then the effective length could be determined as:

$$h_e = 2R. \tag{32}$$

For the case of short nanorods ($H < 4R$), the effective length is simply set to:

$$h_e = \frac{H}{2}. \tag{33}$$

The shape function to be determined in Eq. (31) should be agreeable to the curve trend shown in Fig. 6, which is also schematically shown in Fig. 5. The shape function at the initial stage ($z < h_e$) of the left end behaves similarly to an exponential function. In the plateau of the middle region, it can be simply set to 1 because the image force of the nanorod overlaps with that of the nanowire. The region of the right end is symmetric with the left end. At last, it is sufficient to describe the shape function just with the region at the initial stage ($z < h_e$) of the left end, which could be proposed as a general exponential function:

$$g(z) = ae^{bz} + c, \tag{34}$$

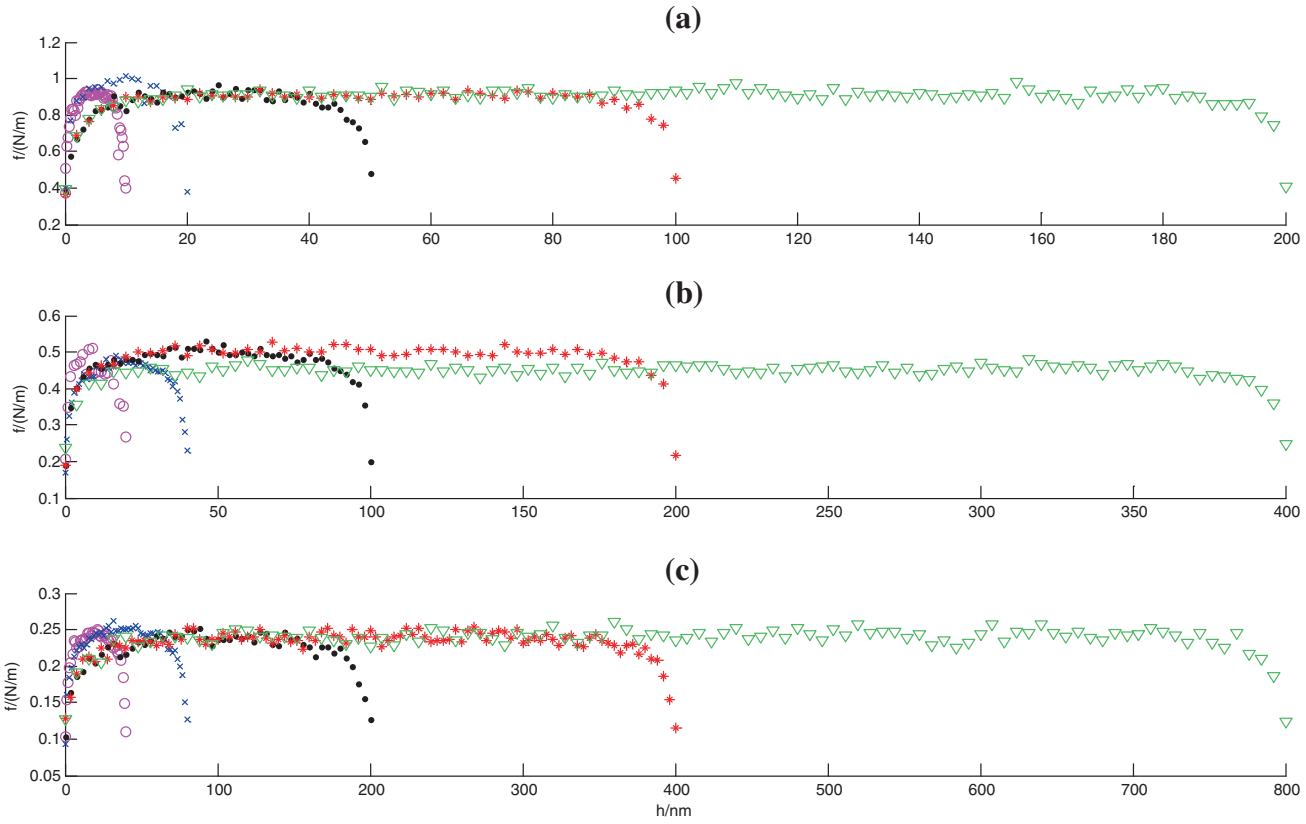

Fig. 6. Image forces for nanorods with different radius and height (a. $R = 10$ nm; b. $R = 20$ nm; c. $R = 40$ nm).

Table 1
Comparison of image forces in finite element analysis and the classical analytical solution.

R (nm)	FEM result (N/m)	Classical analytical result (N/m)	Ratio
10	0.9	0.5305	1.696
20	0.5	0.2653	1.885
40	0.24	0.1326	1.810

Table 2
Curve fitting of the shape function.

R	H	a	b	c	R-square
10	50	−0.5574	−3.6580	0.9936	0.9728
	100	−0.5762	−4.0310	0.9964	0.9878
	200	−0.5365	−3.9540	0.9792	0.9947
20	100	−0.5922	−6.0360	0.9990	0.9695
	200	−0.5851	−4.8300	0.9582	0.9785
	400	−0.4846	−4.0210	1.0280	0.9855
40	200	−0.5022	−3.8250	0.9693	0.9345
	400	−0.4399	−3.7800	0.9823	0.9522
	800	−0.4459	−3.3160	0.9870	0.9467
Average		−0.5244	−4.1612	0.9881	0.9691

where a, b and c are the unknown variables to be fitted with the finite element data.

Table 2 shows the curve fitting results of the shape function. For all the nanorods of different radius and height, the fitted values of a, b and c are consistent and the R-square values are also acceptable.

With the obtained shape function, the final analytical solution to the image force for 3D isotropic finite cylinder is given as:

$$f = \gamma f_0 \times g(z), \tag{35}$$

where γ is the correction factor by calibrating with the finite element data; f_0 is the corresponding image force of the nanowire with surface stress and it has been provided by Eq. (29); $g(z)$ is the shape function consisting of only z coordinate and it is given in Eq. (34) by curve fitting of the finite element data.

Fig. 7 shows the comparison of image forces in 3D isotropic nanorods between the original finite element result without surface stress and the analytical results with and without surface stress. Although the finite element result has some fluctuations due to the precision of the numerical calculation, the curve trend agrees well with the analytical result without surface stress. This turns out to be as expected since the shape function is fitted to the original finite element data. In case that surface stress is considered, image forces generally increase for negative surface elasticity and decrease with positive surface elasticity. In this case, the surface with negative surface elasticity resembles a "soft" media compared to the bulk material and it becomes "rigid" with positive surface elasticity. It can be also seen from Fig. 7 that surface stress plays a more important role in thinner nanorods (R = 10 nm) and it diminishes as the radius of the nanorod increases. In fact, surface stress has little contribution to the final

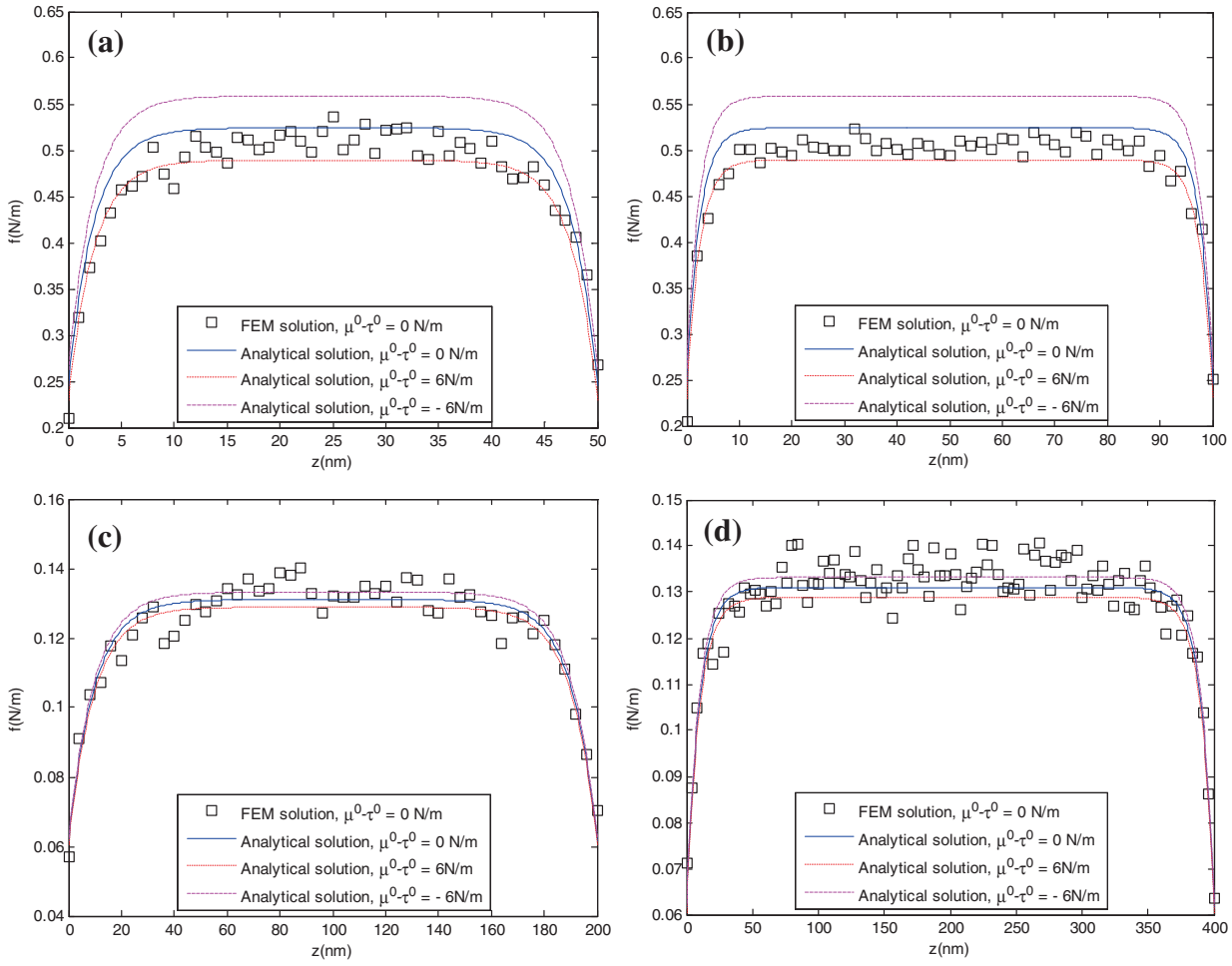

Fig. 7. Comparison of image forces in 3D isotropic nanorods (a. R = 10 nm, H = 50 nm; b. R = 10 nm, H = 100 nm; c. R = 40 nm, H = 200 nm; d. R = 40 nm, H = 400 nm).

image force when the radius of the nanorod is around 50 nm and above, which is also seen in the case of nanowires in Fig. 3.

6. Conclusions

This work provides alternative analytical formulations of image forces for nanowires which are in more flexible forms compared with the infinite power series solutions from complex variable method. Moreover, this work proposes analytical formulations of image forces for nanorods (3D) by approximating the 3D shape effect as a height-dependent shape function, which is obtained through curve fitting of the finite element results of image forces without surface stress. The analytical formulation of nanorods has not been found in other literatures so far. The results of nanowires are demonstrated to be acceptable compared with the classical solution and complex variable method under most circumstances except the case of positive surface elasticity and the deviation only happens when the dislocation is close to the surface and the radius of the nanowire is extremely small. This work could contribute to nanostructure design and provide guidance for the fabrication of high quality nanostructures.

Acknowledgements

This work is supported and funded by Georgia Institution of Technology from USA and Georgia Tech Lorraine, CNRS, Region Lorraine from France.

References

Ahmadzadeh-Bakhshayesh, H., Yu Gutkin, M., Shodja, H., 2012. Surface/interface effects on elastic behavior of a screw dislocation in an eccentric core–shell nanowire. International Journal of Solids and Structures 49, 1665–1675.
Aifantis, E.C., 2003. Update on a class of gradient theories. Mechanics of Materials 35, 259–280.
Aifantis, E.C., 2009. Non-singular dislocation fields. In: Cai, W., Edagawa, K., Ngan, A.H.W. (Eds.), Dislocations, 2008.
Aifantis, E.C., 2011. On the gradient approach – relation to Eringen's nonlocal theory. International Journal of Engineering Science 49, 1367–1377.
Aifantis, K.E., Askes, H., 2007. Gradient elasticity with interfaces as surfaces of discontinuity for the strain gradient. Journal of the Mechanical Behavior of Materials 18, 283–306.
Aifantis, K.E., Kolesnikova, A.L., Romanov, A.E., 2007. Nucleation of misfit dislocations and plastic deformation in core/shell nanowires. Philosophical Magazine 87, 4731–4757.
Colby, R., Liang, Z., Wildeson, I.H., Ewoldt, D.A., Sands, T.D., García, R.E., Stach, E.A., 2010. Dislocation filtering in GaN nanostructures. Nano Letters 10, 1568–1573.
Davoudi, K.M., Gutkin, M.Y., Shodja, H.M., 2009. Analysis of stress field of a screw dislocation inside an embedded nanowire using strain gradient elasticity. Scripta Materialia 61, 355–358.
Davoudi, K.M., Gutkin, M.Y., Shodja, H.M., 2010. A screw dislocation near a circular nano-inhomogeneity in gradient elasticity. International Journal of Solids and Structures 47, 741–750.
Dingreville, R., Qu, J., Cherkaoui, M., 2005. Surface free energy and its effect on the elastic behavior of nano-sized particles, wires and films. Journal of the Mechanics and Physics of Solids 53, 1827–1854.
Du, D., Srolovitz, D.J., 2004. Faceted dislocation surface pits. Acta Materialia 52, 3365–3374.
Dundurs, J., Mura, T., 1964. Interaction between an edge dislocation and a circular inclusion. Journal of the Mechanics and Physics of Solids 12, 177–189.
Dundurs, J., Sendeckyj, G., 1965. Edge dislocation inside a circular inclusion. Journal of the Mechanics and Physics of Solids 13, 141–147.
Eringen, A.C., 1977. Edge dislocation in nonlocal elasticity. International Journal of Engineering Science 15, 177–183.
Eringen, A.C., 1984. On continuous distributions of dislocations in nonlocal elasticity. Journal of Applied Physics 56, 2675–2680.
Eringen, A.C., 2001. Screw dislocation in non-local elasticity. Journal of Physics D: Applied Physics 10, 671.
Eshelby, J.D., 1953. Screw dislocations in thin rods. Journal of Applied Physics 24, 176–179.
Fang, Q.H., Liu, Y.W., 2006a. Size-dependent elastic interaction of a screw dislocation with a circular nano-inhomogeneity incorporating interface stress. Scripta Materialia 55, 99–102.
Fang, Q.H., Liu, Y.W., 2006b. Size-dependent interaction between an edge dislocation and a nanoscale inhomogeneity with interface effects. Acta Materialia 54, 4213–4220.
Gurtin, M.E., Ian Murdoch, A., 1975. A continuum theory of elastic material surfaces. Archive for Rational Mechanics and Analysis 57, 291–323.
Gurtin, M.E., Weissmuller, J., Larche, F., 1998. A general theory of curved deformable interfaces in solids at equilibrium. Philosophical Magazine A 78, 1093–1109.
Gutkin, M.Y., Mikaelyan, K.N., Aifantis, E.C., 2000. Screw dislocation near interface in gradient elasticity. Scripta Materialia 43, 477–484.
Hirth, J.P., Lothe, J., 1982. Theory of Dislocations. John Wiley and Sons Inc..
Hull, D., Bacon, D.J., 2011. Introduction to Dislocations. Elsevier Science.
Kröner, E., 1967. Elasticity theory of materials with long range cohesive forces. International Journal of Solids and Structures 3, 731–742.
Lazar, M., Maugin, G.A., 2006. Dislocations in gradient elasticity revisited. Proceedings of the Royal Society A: Mathematical, Physical and Engineering Science 462, 3465–3480.
Lazar, M., Maugin, G.A., Aifantis, E.C., 2006. Dislocations in second strain gradient elasticity. International Journal of Solids and Structures 43, 1787–1817.
Liang, Z., Colby, R., Wildeson, I.H., Ewoldt, D.A., Sands, T.D., Stach, E.A., García, R.E., 2010. GaN nanostructure design for optimal dislocation filtering. Journal of Applied Physics 108, 074313.
Liu, Y.W., Fang, Q.H., 2007. Analysis of a screw dislocation inside an inhomogeneity with interface stress. Materials Science and Engineering: A 464, 117–123.
Liu, X., Golubov, S., Woo, C., Huang, H., 2004. Glide of edge dislocations in tungsten and molybdenum. Materials Science and Engineering A 365, 96–100.
Lubarda, V.A., 2011. Image force on a straight dislocation emitted from a cylindrical void. International Journal of Solids and Structures 48, 648–660.
Luo, J., Xiao, Z., 2009. Analysis of a screw dislocation interacting with an elliptical nano inhomogeneity. International Journal of Engineering Science 47, 883–893.
Luryi, S., Suhir, E., 1986. New approach to the high quality epitaxial growth of lattice-mismatched materials. Applied Physics Letters 49, 140.
Miller, R.E., Shenoy, V.B., 2000. Size-dependent elastic properties of nanosized structural elements. Nanotechnology 11, 139.
Muskhelishvili, N.I., 1977. Some Basic Problems of the Mathematical Theory of Elasticity. Springer.
People, R., Bean, J., 1985. Calculation of critical layer thickness versus lattice mismatch for Ge_xSi_{1-x}/Si strained-layer heterostructures. Applied Physics Letters 47, 322.
Schwarz, K., 1999. Simulation of dislocations on the mesoscopic scale. I. Methods and examples. Journal of Applied Physics 85, 108.
Shodja, H., Davoudi, K., Gutkin, M., 2008. Analysis of displacement and strain fields of a screw dislocation in a nanowire using gradient elasticity theory. Scripta Materialia 59, 368–371.
Shuttleworth, R., 1950. The surface tension of solids. Proceedings of the Physical Society. Section A 63, 444.
Smith, E., 1968. The interaction between dislocations and inhomogeneities—I. International Journal of Engineering Science 6, 129–143.
Srinivasan, S., Geng, L., Liu, R., Ponce, F.A., Narukawa, Y., Tanaka, S., 2003. Slip systems and misfit dislocations in InGaN epilayers. Applied Physics Letters 83, 5187.
Stagni, L., Lizzio, R., 1983. Shape effects in the interaction between an edge dislocation and an elliptical inhomogeneity. Applied Physics A: Materials Science and Processing 30, 217–221.
Stroh, A., 1958. Dislocations and cracks in anisotropic elasticity. Philosophical Magazine 3, 625–646.
Ting, T., Barnett, D., 1993. Image force on line dislocations in anisotropic elastic half-spaces with a fixed boundary. International Journal of Solids and Structures 30, 313–323.
Warren, W.E., 1983. The edge dislocation inside an elliptical inclusion. Mechanics of Materials 2, 319–330.
Ye, W., Paliwal, B., Goh, W.H., Cherkaoui, M., Ougazzaden, A., 2012. Finite element modeling of dislocation in solids and its applications to the analysis of GaN nanostructures. Computational Materials Science 58, 154–161.
Ye, W., Paliwal, B., Ougazzaden, A., Cherkaoui, M., 2013. Analytical close-form solutions to the elastic fields of solids with dislocations and surface stress. Philosophical Magazine 93, 2497–2513.
Zhong, Y., Zhu, T., 2008. Simulating nanoindentation and predicting dislocation nucleation using interatomic potential finite element method. Computer Methods in Applied Mechanics and Engineering 197, 3174–3181.